🔓 **Open Access**

Photonic Microwave Filter With Steep Skirt Selectivity Based on Stimulated Brillouin Scattering

Diego Samaniego
Borja Vidal

✦ **IEEE** **photonics** SOCIETY
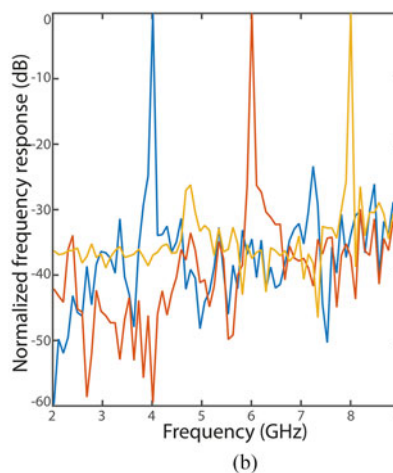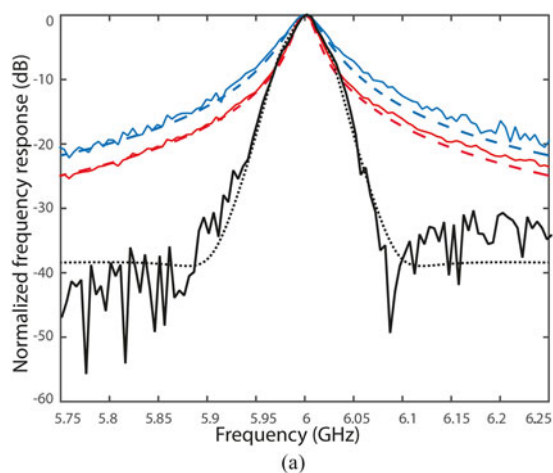
◆ **IEEE**

Photonic Microwave Filter With Steep Skirt Selectivity Based on Stimulated Brillouin Scattering

Diego Samaniego and Borja Vidal

Nanophotonics Technology Center, Universitat Politècnica de València,
Valencia 46022, Spain.

Abstract: A method to enhance the filter slope of Brillouin-based photonic microwave filters is presented. This improvement is achieved by the combination of Brillouin gain and loss responses over phase-modulated signals. The experimental results show passband responses exhibiting a slope of 16.7 dB per octave, which corresponds with a threefold improvement in comparison to the natural Lorentzian response for the same gain.

Index Terms: Microwave photonics, scattering, Fiber non-linear optics, nonlinear effects.

1. Introduction

Filtering is one of the main functions performed in communication systems, radar, and sensing instruments. Although typically performed using electronic circuitry, photonics allows for an alternative implementation [1]. Extensive research has been carried out and different photonic microwave filter architectures have been presented, including transversal filters [2]–[3], comb sources [4], fiber Bragg gratings [5], ring resonators [6], and stimulated Brillouin scattering (SBS) [7]–[10].

Photonic microwave filtering offers several features that are not easily achievable in the microwave/digital domains such as wide bandwidth and tuning range, reconfigurability of the frequency response [2] and the ability of some architectures to be seamlessly combined with radio over fiber distribution links. More importantly, some schemes [6]–[10] can be integrated into a Photonic Integrated Circuit (PIC) to implement photonic analogs of discrete microwave filter devices. Integration is a critical step to compete with implementations in the microwave/digital domains by offering compact low-cost solutions with the potential to avoid the performance degradation in terms of Q-factor suffered by conventional microwave filters when miniaturized. Among the architectures with integration potential, SBS-based schemes are very stable, can exhibit a single bandpass that can be tuned and reconfigured to show flat-top responses and they can easily implement narrow filter responses in the range of MHz to GHz, as opposed to the periodic and rather broadband responses showed by transversal filters.

Microwave filters with competitive specifications typically require flat-top bandpass, strong rejection in the stopband and steep slopes. Flat-top filter responses with good shape factors have
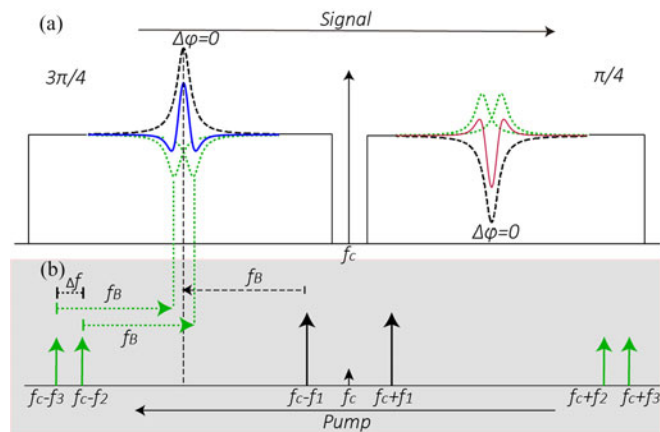
Fig. 1. Principle of operation. (a) Optical spectrum of the forward signal with SBS amplitude gain and loss responses. (b) Backward pump signals with frequency f_p, where p = 1, 2, 3.

been demonstrated using SBS [10] by increasing the SBS gain using two stages in cascade. Unfortunately, the natural gain/loss profile of unsaturated SBS follows a slow-decaying Lorentzian response [12] that results in poor filter slopes.

Here, a technique to enhance the slope of SBS-based photonic microwave filters is demonstrated. The principle of operation is based on combining a SBS gain response with two frequency-offset SBS loss responses that are used to attenuate the slowly decaying tail of the Lorentzian response. When this engineered SBS response is applied to a phase-modulated microwave signal, SBS introduces a gain/loss over the sidebands that breaks the out-of-phase condition between sidebands. Thus, any microwave signal going through the system is eliminated but in the band where the combined SBS response has been applied. The combination of gain and loss responses in SBS has been previously used to reduce the optical Brillouin bandwidth [13] at the cost of severely reducing its gain. Instead, here it is shown both theoretically and experimentally that for a SBS-based microwave filter the slope can be enhanced while keeping the rejection ratio by using phase modulation jointly with a combination of gain and loss responses.

2. Photonic Microwave Filter Architecture

Fig. 1 describes the principle of operation. By means of SBS, a pump counterpropagating the signal induces both a gain and a loss response in amplitude that are up- and down-shifted in frequency (f_B), respectively [12]. The left side of Fig. 1(a) (left) shows how the gain is combined with two loss (notch) responses in amplitude. These notches introduce a sharp drop in the natural Lorentzian tail (dashed blue) as it can be seen in the combined response (black solid) at the cost of a slight reduction of the combined gain. The same happens in the other sideband (Fig. 1(a), right).

To obtain the combined SBS response, three pumps counterpropagating the phase-modulated microwave signal are needed. They are generated using a double-sideband suppressed-carrier (DSB-SC) modulation as shown in Fig 1(b). In the lower band, the three pumps are labelled $f_c - f_1, f_c - f_2, f_c - f_3$, where $f_c - f_1$ induces a Stokes gain wave $P_{g1}(f_c - f_{RF})$ (that generates the central SBS gain, $g_1(f_c - f)$) and the other two pumps: $f_c - f_2$, $f_c - f_3$ induce two Stokes loss waves $P_{\alpha2}(f_c - f_{RF})$, $P_{\alpha3}(f_c - f_{RF})$ in the lower band signal (that induce SBS loss, $\alpha_p(f_c - f)$, at the sides of the central SBS gain). Whereas for the upper band, $f_c + f_1$ induce a Stokes loss wave $P_{\alpha1}(f_c + f_{RF})$ and $f_c + f_2, f_c + f_3$ induce two Stokes gain waves $P_{g2}(f_c + f_{RF})$, $P_{g3}(f_c + f_{RF})$. By changing the frequency of the local oscillators used to generate the pumps, the filter response can be tuned.

A theoretical model of the SBS-driven filter response can be obtained. For the sake of simplicity, the case of a single pump is considered first. For this case, both the SBS gain and loss can be
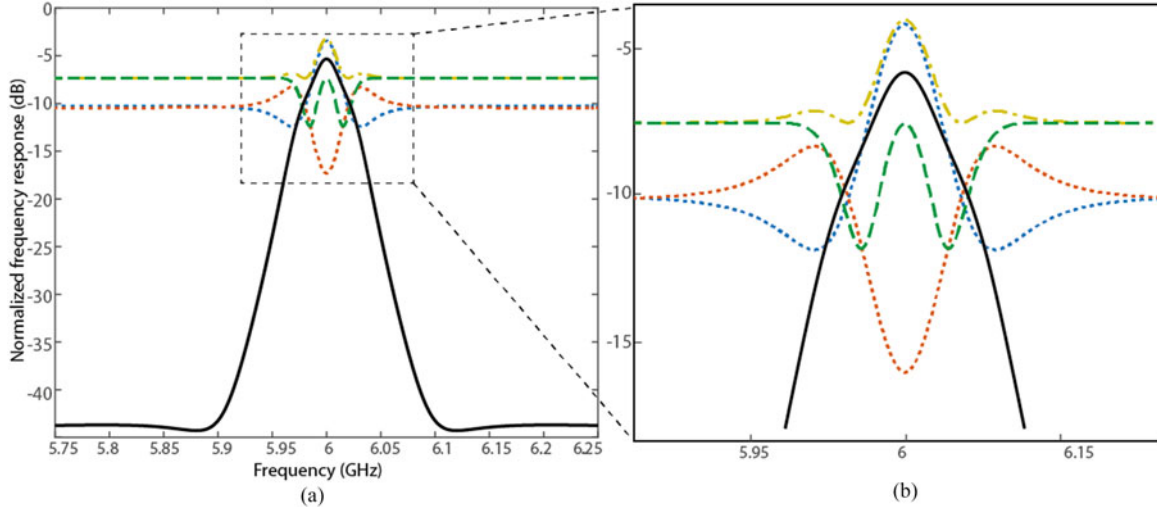
Fig. 2. (a) Evaluation of the terms of (6). (Black solid) Normalized total frequency response of the SBS-based filter obtained from (6). (Blue dotted) Amplitude frequency response of the gain SBS response (lower sideband), i.e. first term of (6). (Red dotted) Amplitude frequency response of the loss SBS response (upper sideband), i.e., second term of (6). (Yellow dot-dashed) Combination of the first and second terms of (6). (Green dashed) third and fourth term of (6). (b) Detail of Fig. 2(a).

described as follows [14]:

$$g_p\left(fc \pm f\right) = \frac{g_o}{2}\frac{\left(\frac{\gamma_B}{2}\right)^2}{\left(-f_p + f_B + f\right)^2 + \left(\frac{\gamma_B}{2}\right)^2} \pm j\frac{g_o}{4}\frac{\gamma_B(-f_p + f_B + f)}{\left(-f_p + f_B + f\right)^2 + \left(\frac{\gamma_B}{2}\right)^2} \quad (1)$$

$$\alpha_p\left(fc \mp f\right) = -\frac{g_o}{2}\frac{\left(\frac{\gamma_B}{2}\right)^2}{\left(-f_p + f_B + f\right)^2 + \left(\frac{\gamma_B}{2}\right)^2} \pm j\frac{g_o}{4}\frac{\gamma_B(-f_p + f_B + f)}{\left(-f_p + f_B + f\right)^2 + \left(\frac{\gamma_B}{2}\right)^2} \quad (2)$$

where g_0 is the Brillouin gain factor, γ_B represents the Brillouin linewidth in the fiber and f_B is the Brillouin frequency shift.

To estimate the SBS gain and loss, the coupled differential equations that define SBS in steady state have to be solved [12]. Here, considering the solution proposed in [15], the spatial distribution of the field intensity is $I_p = P_p/A_{eff}$, where A_{eff} is the effective area, and it is assumed that the losses in the fiber are usually low. Assuming no pump depletion, $P_p(0) = P_p(L) = P_p$, the Stokes gain/loss waves can be expressed as

$$P_{gp}(f_c \pm f_{RF}) = \frac{\left[P_p - P_s\right]}{P_p \exp\left\{gp\left(fc \pm f_{RF}\right)\left[P_p - P_s\right]L\right\} - P_s} \quad (3)$$

$$P_{\alpha p}(f_c \mp f_{RF}) = \frac{\left[P_p - P_s\right]}{P_p \exp\left\{\alpha p\left(fc \mp f_{RF}\right)\left[P_p - P_s\right]L\right\} - P_s} \quad (4)$$

where P_p is the signal pump, and P_s is the signal power at the fiber input $z = 0$.

The filter frequency response with a single SBS pump can be derived using the small signal approximation and omitting the DC component and higher-order harmonics. It is given by [14]

$$|H\left(f_{RF}\right)|^2 = \frac{P_{RFout}}{P_{RFin}} = \frac{\pi^2 \Re^2 Z_{in} Z_0 P_0^2 \alpha_0^2}{4V_\pi^2}\left[\left|P_{gp}(f_c - f_{RF})\right|^2 + \left|P_{\alpha p}(f_c + f_{RF})\right|^2\right.$$

$$\left. - P_{gp}(f_c - f_{RF})(P_{\alpha p}(f_c + f_{RF}) - P_{gp}(f_c - f_{RF})^*(P_{\alpha p}(f_c + f_{RF})^*\right] \quad (5)$$
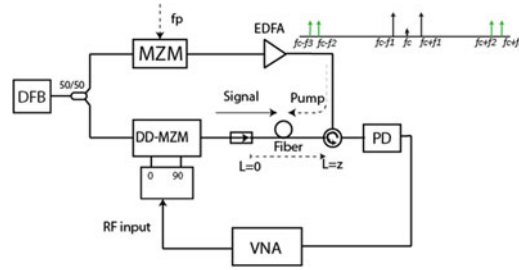
Fig. 3. Block diagram of the experimental setup. DFB: distributed feedback laser, MZM: Mach-Zehnder modulator, DD-MZM: Dual-Drive MZM, VNA: vector network analyzer.

where P_{RFout} is the RF power at the output of PD, P_{RFin} is the RF power at the input, as shown in Fig. 3, $\Re$ is the PD responsivity, Z_0 is the load resistance, P_0 is the optical power of the light, Z_{in} is the input impedance of the DD-MZM, and α_0 is the optical loss between the laser output and the PD input.

When additional pumps are present, the filter response can be obtained from (5). In particular, for the case of three Stokes gain/loss waves, the filter response can be described by (6) when phase modulation is used taking into account that, in the lower sideband of the signal, there are three interacting signals $P_{g1}(f_c - f_{RF})$, $P_{\alpha2}(f_c - f_{RF})$, $P_{\alpha3}(f_c - f_{RF})$, whereas in the upper sideband of the signal the interaction is produced by another three terms: $P_{\alpha1}(f_c + f_{RF})$, $P_{g2}(f_c + f_{RF})$, $P_{g3}(f_c + f_{RF})$.

$$|H(f_{RF})|^2 = \frac{\pi^2 \Re^2 Z_{in} Z_0 P_0^2 \alpha_0^2}{4 V_\pi^2}$$

$$\left[|P_{g1}(f_c - f_{RF})|^2 \, |P_{\alpha2}(f_c - f_{RF})|^2 \, |P_{\alpha3}(f_c - f_{RF})|^2 \right.$$

$$+ \, |P_{\alpha1}(f_c + f_{RF})|^2 \, |P_{g2}(f_c + f_{RF})|^2 \, |P_{g3}(f_c + f_{RF})|^2$$

$$- \, P_{g1}(f_c - f_{RF}) P_{\alpha2}(f_c - f_{RF}) \, P_{\alpha3}(f_c - f_{RF})$$

$$P_{\alpha1}(f_c + f_{RF}) P_{g2}(f_c + f_{RF}) P_{g3}(f_c + f_{RF})$$

$$- \, P_{g1}(f_c - f_{RF})^* \, P_{\alpha2}(f_c - f_{RF})^* P_{\alpha3}(f_c - f_{RF})^*$$

$$\left. P_{\alpha1}(f_c + f_{RF})^* \, P_{g2}(f_c + f_{RF})^* \, P_{g3}(f_c + f_{RF})^* \right]. \tag{6}$$

Unlike single sideband amplitude modulation, given by the first term of (6), phase modulation results in the subtraction of several terms that lead to partial cancellation of the long decaying tails of Brillouin response. Fig. 2 shows this effect. The figure shows the total theoretical filter response (black solid line) for the interaction of three gain/loss waves with a phase modulated signal, as given by (6), as well as the contribution of each term of the equation. The first term of (6) (blue dotted in Fig. 2) corresponds with the gain response obtained from the combination of the Brillouin gain with two notches. This gain profile is applied on the lower sideband of the signal and shows an enhanced slope in comparison to the natural gain Lorentzian response of SBS (as it can be seen in Fig. 1, blue solid). This first term (blue dotted) corresponds to single sideband modulation, as in [13]. On the other hand, the second term (red dotted in Fig. 2) corresponds to the loss response obtained from the combination of the natural Brillouin loss with two gain profiles at the sides, which can also be seen in the upper sideband of Fig. 1 (red solid). These two modified SBS responses are generated in the optical domain. However, after photodetection, a third and a fourth terms appear (their sum is shown in green dashed in Fig. 2) which depend on the phase information of all Stokes waves. Equation (6) shows that the first and second terms are added together (Stokes gain + Stokes loss) (showed as the yellow dot-dashed line in Fig. 2), whereas the third and fourth term have the opposite sign. This latter two terms introduce a small reduction on the gain of the filter passband but, on the positive side, they cancel the Lorentzian tail and improve the filter selectivity.
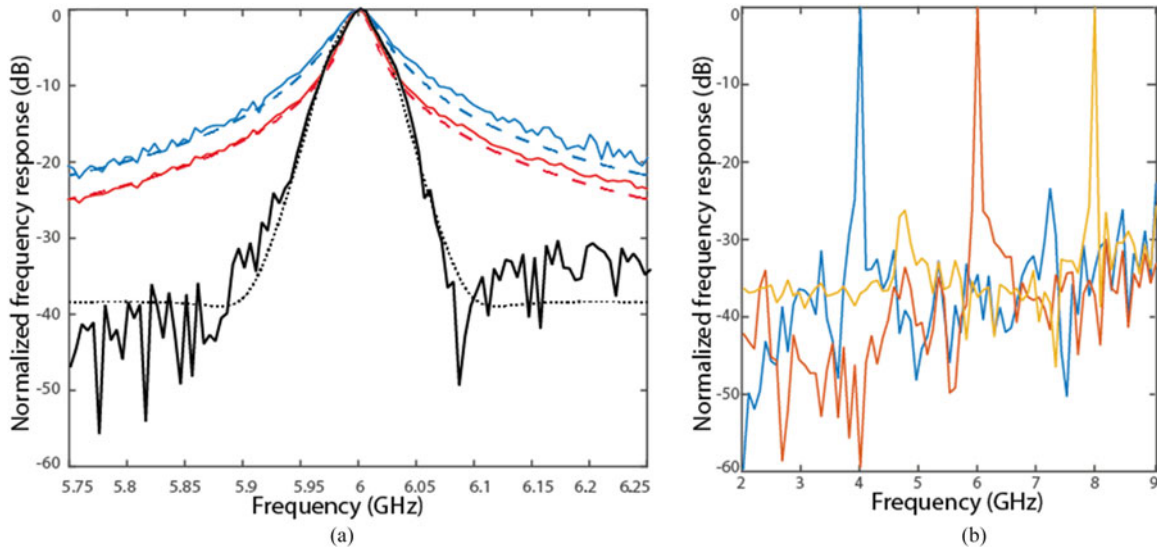
Fig. 4. (a) (Black solid) Normalized RF frequency response of the SBS-based filter. (Black dashed) theoretical filter response obtained from equation (6) with $f_1 = 15.64$ GHz, $f_2 = 3.62$ GHz, $f_3 = 3.66$ GHz. (Blue dashed) theoretical filter response with a single pump (5) and natural gain of 5 dB. (Blue solid) experimental filter response with a single pump and natural gain of 5 dB with $f_1 = 15.64$ GHz; (red dashed) theoretical filter response with a single pump (5) and SBS natural gain of 15 dB. (Red solid) experimental filter response with a single pump and natural gain of 5 dB with $f_1 = 15.64$ GHz. (b) Normalized frequency response of the SBS-based tunable filter.

Key design parameters are the values of f_2 and f_3, which have to be chosen to optimize the slope of the slow-decaying Lorentzian tail of the gain response while minimizing the reduction of the gain of the passband. In amplitude modulation, the loss responses induce a reduction on both bandwidth and gain with no enhancement on selectivity. Unlike this, phase modulation induces a smaller change of bandwidth but with a steeper slope. The tunability of the central frequency of the filter response is bounded by the bandwidth of the electrooptic components and the tuning range of the three local oscillators.

3. Experimental Results

Fig. 3 shows the experimental setup used to validate the concept. The light from a DFB source at 1548 nm with an ouput power of 10 dBm, was divided by a directional coupler 50/50. The upper path of the setup was used to generate the pump while the lower one corresponds to the signal. In the upper path, the light entered a 40 GHz intensity modulator (MZM) biased at minimum transmission (MITB), generating a DSB-SC modulation. The pump signal f_p, had three components, which induce one gain and two loss responses over the lower sideband and the opposite f_p for the upper sideband. The pump waves were generated using a vector signal generator (Agilent ESG E4438C) and a signal generator (Rohde & Schwarz SMR 20). The particular frequencies and amplitudes of these signals were obtained from simulations performed with the model described in Section 2. Optical amplification (40 dB) was used to boost the pump signal and, finally, an optical circulator directed the pump signal to the nonlinear medium (a reel of 1 km-long HNLF with Brillouin linewidth $\gamma_B = 40$ MHz and Brillouin frequency shift $f_B = 9.64$ GHz). In the lower path, the data signal was phase modulated using a 40 GHz dual-drive optical modulator (DD-MZM) and a 2-18 GHz hybrid 90° coupler [14], [16]. The DD-MZM was biased at 9.7 V [maximum transmission point (MATB)] The DC half-wave voltage of the DD-MZM was measured to be 5.4 V.

Unlike [14], where it was used to dynamically switch between bandpass and notch filter responses, we just used a DD-MZM for phase modulation due to the unavailability of a phase modulator in our laboratory. The modulated signal passed back through the HNLF and reached a PIN photodiode
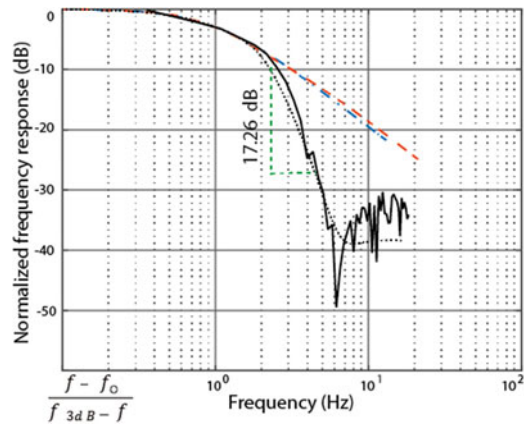
Fig. 5. Bode diagram of the SBS-based filter response. Experimental filter response (black solid) with 16.7 dB/oct; theoretical filter response obtained from (6) (black dotted) with 17.26 dB/oct; theoretical response with a single pump and 5 dB gain (blue dash-dotted) with 3.79 dB/oct; theoretical response with a single pump and 15 dB gain (red dashed) with 4.08 dB/oct.
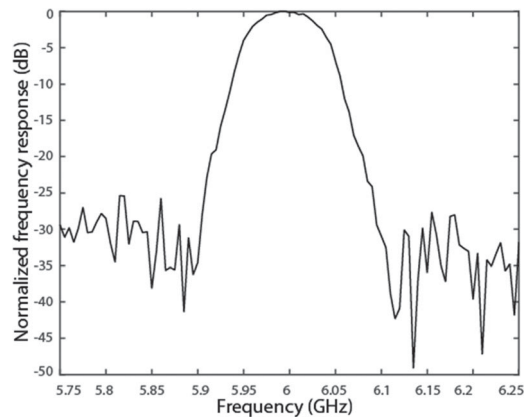

Fig. 6. Normalized RF frequency response of the SBS-based filter with 84 MHz FWHM bandwidth.

with a bandwidth from 30 KHz to 9 GHz. Finally, the frequency response of the filter was measured with a vector network analyser (VNA, HP 8510C).

The microwave filter response was measured as shown in Fig. 4(a) (black solid). The experimental result showed good agreement with the theoretical model (6). For the sake of comparison, the filter responses obtained directly applying a single pump [7] have been included for two cases with the same pump power at f_1. In the first case, using $f_c - f_1$, $f_c + f_1$, the SBS gain reaches 15 dB, and in the second case, applying the proposed method, SBS gain reaches 5 dB, where the gain was measured when the modulator signal DD-MZM acted as a lower side band carrier with LSB+C ($V_{bias} = 3\pi/2$). From the comparison shown in Fig. 4(a), it can be seen that in both cases (SBS natural gain of 15 dB and 5 dB), the selectivity is improved. The tradeoff between the filter gain, bandwidth and slope can be modified by changing the frequencies of the pumps as well as their amplitudes. Figure 4(b) show the tuning capability of the filter by changing the frequency of the microwave oscillators.

By mapping the bandpass filter response to a lowpass function, the slope response can be estimated (see Fig. 5). The figure shows a three-fold enhancement of the slope, reaching 16.7 dB/oct in comparison to the 6 dB/oct from single pump responses (single pole filter response) [17]. A third-order filter has been implemented as corresponds to the combination of a bandpass and two notch responses in cascade [18].

Additionally, a filter with a flat-top response has been obtained by sweeping the pump frequency and including a feedback algorithm [11] to control the sweeping gain pump. The experimental response is shown in Fig. 6. The 3 dB bandwidth is 84 MHz with a slope of around 18 dB/oct. Since the technique only produce an effect on the tails of the response, it does not introduce any particular limitation to the filter bandwidth.

Finally, the noise degradation introduced by SBS filtering was analyzed. Measurements show that the signal to noise ratio is degraded in 5 dB when the SBS-filter is used.

4. Conclusion

It has been shown both through a theoretical model and experiments that phase modulation induces a cancellation on the Lorentzian tails when a combination of gain and loss Brillouin responses are applied to implement a SBS-based photonic microwave filter. This results in enhanced selectivity of the filter response. The method does not require high gain and therefore the noise figure of the link is barely affected. At the same time, due to this fact, the approach is suitable to be exploited in Photonic Integrated Circuits (PIC) for microwave processing [8] since given their short interaction length, little gain can be obtained. Further work is needed to further enhance selectivity in order to match filter specification masks and pave the way towards integrated photonic microwave filters competitive with standard microwave implementations.

References

[1] J. Yao, "Photonics to the rescue: A fresh look at microwave photonic filters," *IEEE Microw. Mag.*, vol. 16, no. 8, pp. 46–60, Sep. 2015.
[2] B. Vidal, M. A. Piqueras, and J. Martí, "Photonic microwave filter based on spectrum slicing with reconfiguration capability," *Electron. Lett.*, vol. 41, no. 23, pp. 1286–1287, 2005.
[3] B. Vidal, J. L. Corral, and J. Martí, "All-optical WDM multi-tap microwave filter with flat bandpass," *Opt. Exp.*, vol. 14, no. 2, pp. 581–586, 2006.
[4] V. R. Supradeepra *et al.*, "Comb-based radiofrequency photonic filters with rapid tunability and high selectivity," *Nature Photon.*, vol. 6, no. 3, pp. 186–194, 2012.
[5] J. Palací *et al.*, "Tunable photonic microwave filter with single bandpass based on a phase-shifted fiber bragg grating," *IEEE Photon. Technol. Lett.*, vol. 22, no. 19, pp. 1467–1469, Oct. 2010.
[6] M. S. Rasras *et al.*, "Demonstration of a tunable microwave-photonic notch filter using low-loss silicon ring resonators," *J. Lightw. Technol.*, vol. 27, no. 12, pp. 2105–2110, Jun. 2009.
[7] B. Vidal, M. A. Piqueras, and J. Martí, "Tunable and reconfigurable photonic microwave filter based on stimulated Brillouin scattering," *Opt. Lett.*, vol. 32, no. 1, pp. 23–25, 2007.
[8] A. Byrnes *et al.*, "Photonic chip based tunable and reconfigurable narrowband microwave photonic filter using stimulated Brillouin scattering," *Opt. Exp.*, vol. 20, no. 17, pp. 18836–18845, 2012.
[9] Y. Stern *et al.*, "Tunable sharp and highly selective microwave-photonic band-pass filters based on stimulated Brillouin scattering," *Photon. Res.*, vol. 2, no. 4, pp. B18–B25, 2014.
[10] W. Wei, L. Yi, Y. Jaouën, and W. Hu, "Bandwidth-tunable narrowband rectangular optical filter based on stimulated Brillouin scattering in optical fiber," *Opt. Exp.*, vol. 22, no. 19, pp. 23249–23260, 2014.
[11] W. Wei, L. Yi, Y. Jaouën, and M. Morvan, "Brillouin rectangular optical filter with improved selectivity and noise performance*," IEEE Photon. Technol. Lett.*, vol. 27, no. 15, pp. 1593–1596, Aug. 2015.
[12] G. P. Agrawal, *Nonlinear Fiber Optics*. New York, NY, USA: Academic, 2007.
[13] S. Preußler, A. Wiatrek, K. Jamshidi, and T. Schneider, "Brillouin scattering gain bandwidth reduction down to 3.4 MHz," *Opt. Exp.*, vol. 19, no. 9, pp. 8565–8570, 2011.
[14] W. Zhang and R. A. Minasian, "Switchable and tunable microwave photonic Brillouin-based filter," *IEEE Photon. J.*, vol. 4, no. 5, pp. 1443–1455, Oct. 2012.
[15] L. Chen and X. Bao, "Analytical and numerical solutions for steady state stimulated Brillouin scattering in a single-mode fiber," *Opt. Commun.*, vol. 152, no. 1, pp. 65–70, 1998.
[16] X. Han and J. Yao, "Bandstop-to-bandpass microwave photonic filter using a phase-shifted fiber Bragg grating," *J. Lightw. Technol.*, vol. 33, no. 24, pp. 5133–5139, Dec. 2015.
[17] B. P. Lathi, *Linear Systems and Signals*. New York, NY, USA: Oxford Univ. Press, 2005.
[18] H. Zumbahlen, *Linear Circuit Design Handbook*. Burlington, MA, USA: Newnes, 2011.